

## Research Article

# Oil-Based Drilling Fluid Plugging Method for Strengthening Wellbore Stability of Shale Gas

Pengcheng Wu,<sup>1</sup> Chengxu Zhong,<sup>1</sup> Zhengtao Li,<sup>1</sup> Zhen Zhang,<sup>1</sup> Zhiyuan Wang ,<sup>2</sup>  
and Weian Huang <sup>2,3</sup>

<sup>1</sup>Shale Gas Research Institution of PetroChina Southwest Oil & Gas Field Company, Chengdu, 610056 Sichuan, China

<sup>2</sup>School of Petroleum Engineering, China University of Petroleum (East China), Qingdao, Shandong 266580, China

<sup>3</sup>Key Laboratory of Unconventional Oil and Gas Development, Ministry of Education (China University of Petroleum (East China)), Qingdao, Shandong 266580, China

Correspondence should be addressed to Weian Huang; [masterhuang1997@163.com](mailto:masterhuang1997@163.com)

Received 3 November 2020; Revised 3 January 2021; Accepted 27 January 2021; Published 17 February 2021

Academic Editor: Guanglong Sheng

Copyright © 2021 Pengcheng Wu et al. This is an open access article distributed under the Creative Commons Attribution License, which permits unrestricted use, distribution, and reproduction in any medium, provided the original work is properly cited.

Finding out the reasons for wellbore instability in the Longmaxi Formation and Wufeng Formation and putting forward drilling fluid technical countermeasures to strengthen and stabilize the wellbore are very crucial to horizontal drilling. Based on X-ray diffraction, electron microscope scanning, linear swelling experiment, and hot-rolling dispersion experiment, the physicochemical mechanism of wellbore instability in complex strata was revealed, and thus, the coordinated wellbore stability method can be put forward, which is “strengthening plugging of micropores, inhibiting filtrate invasion, and retarding pressure transmission.” Using a sand bed filtration tester, high-temperature and high-pressure plugging simulation experimental device, and microporous membrane and other experimental devices, the oil-based drilling fluid treatment agent was researched and selected, and a set of an enhanced plugging drilling fluid system suitable for shale gas horizontal well was constructed. Its temperature resistance is 135°C and it has preferable contamination resistibility (10% NaCl, 1% CaCl<sub>2</sub>, and 8% poor clay). The bearing capacity of a 400 μm fracture is 5 MPa, and the filtration loss of 0.22 μm and 0.45 μm microporous membranes is zero. Compared with previous field drilling fluids, the constructed oil-based drilling fluid system has a greatly improved plugging ability and excellent performance in other aspects.

## 1. Introduction

At present, China’s shale gas exploration and development is at a rapid development stage, and great breakthroughs have been made in the marine shale of the Ordovician Wufeng Formation-Silurian Longmaxi Formation in Sichuan Basin [1]. Jiaoshiba, Changning-Weiyuan, and other atmospheric fields of 100 billion cubic meters have been proven, and the shale gas output has reached  $78 \times 10^8 \text{ m}^3$  in 2016. South Sichuan is a block with the richest shale gas resources and the most realistic development in China. In the drilling process of shale gas horizontal wells in the Changning block, affected by the hydration expansion of shale and the development of rock microcracks, the wall spalling is serious, resulting in complex accidents such as sticking and lost circulation,

which brings great economic losses to drilling operations [2, 3].

The instability of the wellbore is mainly affected by geology, interaction between the shale and drilling fluid, drilling technology, and other factors [4, 5]. The study on the mechanism and countermeasures to wellbore instability has gone through the stages of mechanical and chemical research and to the present stage of mechanical-chemical coupling research [6, 7]. In his article, Dreley [8] described the instability process of hard magnetic shale according to the performance characteristics of hard and brittle shale before and after interaction with water. Based on anisotropic strength theory, Chen et al. [9, 10] studied the influence of anisotropic strength of fractured rock mass on wellbore stability and analysed wellbore stability under isotropic and anisotropic stress

states after mud infiltrated into the fracture. Zhang [11] took the influence of bedding and anisotropy into consideration and established an improved wellbore stability evaluation model. The model took into account the characteristics of rock compressive strength changing with time and developed an evaluation method based on logging data. Gaede et al. [12] found that the strain coefficients of rocks are not equal, which was confirmed by comparing the numerical solutions and analytical solutions in many cases. At the same time, it is proposed to use a thick-walled cylinder with interlayer to carry out simulation experiments in the laboratory, to establish a modified failure quasimeasurement, and to determine the required mud density combined with in situ stress and formation pore pressure. Zhao et al. [13, 14] came up with two ways to solve the borehole wall problem: enhancing the plugging performance of oil-based drilling fluid and reducing the filtration loss at high temperature and high pressure. Tang et al. [15–17] developed a new type of strong plugging oil-based drilling fluid system through an orthogonal test aimed at the problems of the Longmaxi Formation.

At present, there is little research on evaluation and optimization of the plugging agent and construction of a drilling fluid system in the Changning block [18–21]. Therefore, by studying the wellbore instability mechanism of the Longmaxi Formation and Wufeng Formation, this paper selected the oil-based drilling fluid treatment agent and targeted to optimize the micro-nanoplugging agent and further constructed a drilling fluid system with strong plugging and high lubricating oil base to reduce the incidence of complex accidents in the horizontal section of the Longmaxi Formation.

## 2. Materials and Methods

**2.1. Materials.** Rock samples of black shale were taken from the Longmaxi Formation in the Changning block, China. The organic bentonite used to make drilling fluid was purchased from Baker Hughes. As known to all, to design a drilling fluid, various chemical additives are needed. The names of these chemical additives and their manufacturers are summarized in Table 1.

EM-SL main emulsifier is a kind of surfactant with many kinds of surface active groups, which is designed by molecular structure and synthesized artificially. It has a good emulsifying effect and can form stable water-in-oil emulsion. When used in combination with an auxiliary emulsifier, it has good adaptability at 40–200°C, and its density can reach 0.92–2.30 g/cm<sup>3</sup>.

The FR-BK fluid loss additive is a high molecular polymer which is designed by molecular structure and artificially synthesized at high temperature, and its molecular thermal decomposition temperature is as high as 180°C. Good compatibility with other oil-based drilling fluid additives, which can effectively control the water loss of an oil-based drilling fluid at high temperature and high pressure and can also greatly reduce the damage of organic soil submicron particles to low permeability reservoirs.

Lignite-SL is a kind of coal, which contains 20%–80% humic acid. Humic acid is not a single compound but a mixture of compounds with different molecular sizes and differ-

ent structural compositions. These compounds have a skeleton containing aromatic rings, which can be connected by alkylene, carbonyl, ether, or imine groups. There are many carboxyl groups, hydroxyl groups, and sometimes methoxy groups around the aromatic ring.

YX1200 and YX400 are micron plugging agents while drilling, with particle sizes of 1200 meshes and 400 meshes, respectively, which are white powders with unknown composition.

**2.2. X-Ray Diffraction Test (XRD).** X-ray diffraction is used to analyse the mineral components of rock samples. Rock samples need to be crushed to powder which was finer than 150 μm, and then a D/MAX-III A X-ray diffractometer was used for mineralogical analysis. The tube voltage is 40 kV, the tube current is 40 mA, and the scanning range is 2°–30° (step of 0.02°).

**2.3. Scanning Electron Microscopy (SEM).** The square shale slices with a side length of about 5 mm obtained from the Longmaxi Formation were dried at 80°C for 1 d. Their microstructures were determined by scanning electron microscopy (SEM). The SEM measurement was performed using a Quanta™ 650 FEG scanning electron microscope (FEI Corporation, America) at an accelerating voltage of 5 kV.

**2.4. Rheology Tests.** The rheological parameters were measured by using a model ZNN-D6 six-speed rotating viscometer (Qingdao Haitongda Special Instrument Co. Ltd. China). The calculations of AV, PV, and YP are expressed as follows according to the recommended American Petroleum Institute (API) standard.

$$\text{Apparent viscosity (AV)} = \frac{\Phi_{600}}{2} \text{ (mPa}\cdot\text{s)}, \quad (1)$$

$$\text{Plastic viscosity (PV)} = \Phi_{600} - \Phi_{300} \text{ (mPa}\cdot\text{s)}, \quad (2)$$

$$\text{Yield point (YP)} = 0.511(\Phi_{300} - \text{PV}) \text{ (Pa)}, \quad (3)$$

where 300 and 600 are the readings of 300 and 600 rpm, respectively.

**2.5. Linear Swelling Experiment.** The linear swelling experiment was conducted to investigate the swelling behaviour of shale samples immersed in different test fluids. In the experiment, the preparation process of the shale plate was similar to compacted Na-BT in a Na-BT plate soaking test. Firstly, 10 g of the shale samples (screened through a 100-mesh sieve) was compressed to prepare the shale plate. The initial height of the shale plate was recorded. Then, the shale plate was put into the NP-02A linear swell meter (Haitongda Company, Qingdao, China). The oil-based drilling fluid was gently poured into the shale chamber while the initial swelling height was set to zero. Finally, the shale plate was soaked in the test fluids, and the expansion height with time was recorded to calculate the expansion rate.

**2.6. Hot-Rolling Dispersion Experiment.** The hot-rolling dispersion experiment was designed to evaluate the dispersion trend of shale samples after being exposed to different test

TABLE 1: Various chemical additives used in the experiments and corresponding manufacturers.

Chemical additive	Manufacturer	Purity
Emulsifying agent (EM-JH, EM-SL), filtrate reducers (FR-JH, lignite-SL), lubricant (Jiahua)	Jiahua Technology Co., Ltd.	Technical purity
CaCO <sub>3</sub> , NaCl, CaCl <sub>2</sub>	Sinopharm Group Chemical Reagent Co., Ltd.	Analytical purity
Emulsifying agent (EM-XG)	Tianjin Xiongguan Technology Co., Ltd.	Technical purity
Filtrate reducers (FR-BK), N-plugging agent	Baker Hughes	Technical purity
Plugging agent (YX1200, YX400)	Chengdu Xiyouhuawei Science & Technology Co., Ltd.	Technical purity

TABLE 2: Total mineral component analysis of rock samples in the Longmaxi and Wufeng Formations.

Serial number	Well no.	Quartz	Potassium feldspar	Plagioclase	Calcite	Dolomite	Ankerite	Pyrite	Barite	Total clay minerals
1	CN156	28	1	3	19	—	11	3	17	18
2	CN355	41	—	3	13	10	—	3	15	15
3	CN194	35	3	9	14	—	5	3	15	16
4	CN419	38	—	3	18	6	5	5	11	14
5	CN62	35	3	9	14	2	3	5	12	17
6	CN222	37	1	3	9	—	7	3	21	19
7	CN137	21	2	4	27	—	5	3	18	20

TABLE 3: Relative content analysis of clay minerals of rock samples in the Longmaxi and Wufeng Formations.

Serial number	Well no.	Chlorite (Ch)	Illite (I)	Interlayer between Iran and Mongolia (I/S)	Interlayer ratio (%)
1	CN156	10	50	40	20
2	CN355	6	70	24	20
3	CN194	24	49	27	20
4	CN419	16	58	26	20
5	CN62	21	60	19	20
6	CN222	20	63	17	20
7	CN137	33	51	16	20

fluids. Firstly, 50 g of the shale samples (sized 2.00-3.35 mm) and 350 mL oil-based drilling fluid were poured into a sealed container. Then, the sealed container was heated in an XGRL-4 type roller oven (Haitongda Company, Qingdao, China) at 125°C for 16 h. Following hot rolling, the shale samples were filtered by a 40-mesh sieve. The recovered shale samples were cleaned with fresh water and dried at 105°C for 4 h. Finally, the weight of the remaining shale samples was measured to calculate the recovery rate.

**2.7. Sand Bed Filtration Experiment.** The sealing ability of the oil-based drilling fluid can be demonstrated using the sand bed invasion test (Labenski et al. (2003); Reid and Santos (2003)). Approximately 200 grams of 80-100-mesh sieve fine sand was placed in the cell to replace the filter paper. The

pore throats in different grades of sands (40/60 frac sand) can be extrapolated to microfractured formations. The sealing test of drilling fluid was conducted at 25°C, 3.5 MPa.

**2.8. Stability.** The stability of colloid, foam, and suspension was quantitatively evaluated with a Turbiscan stability analyser (Formulation Company, France) (Wiśniewska (2010); Kang et al. (2011)).

**2.9. High-Temperature and High-Pressure Plugging Simulation Experiment.** In this experiment, a high-temperature and high-pressure (HTHP) plugging simulation experimental device is used, which has the characteristics of simple operation and small experimental error, and the simulated conditions are closer to the actual downhole conditions.

The HTHP plugging simulation experiment device is mainly composed of a clamp, a plugging kettle, a pressurizing system, a temperature control system and a stirring system and mainly simulates the plugging effect of the plugging agent on the fracture module under different temperature and pressure conditions. The pressure difference simulation can be realized by the pressure difference between the two ends of the fracture module. The lower end of the fracture module is directly communicated with the atmosphere by the valve stem, and the upper end of the fracture module provides pressure to the kettle body by the nitrogen bottle. At this time, the simulated pressure difference is the pressure provided by the nitrogen bottle to the kettle body.

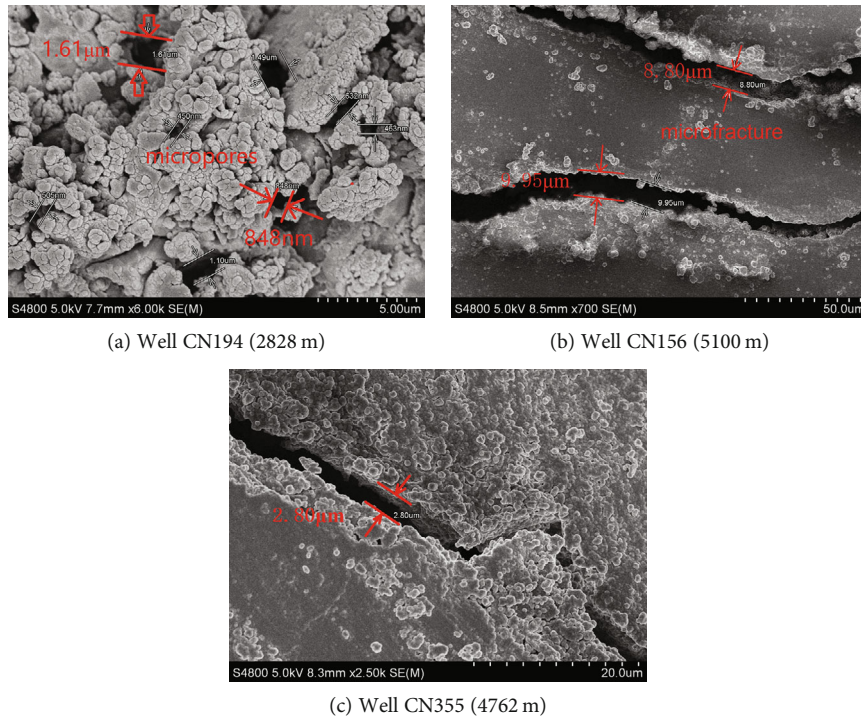


FIGURE 1: SEM images of rock samples of Longmaxi Formation.

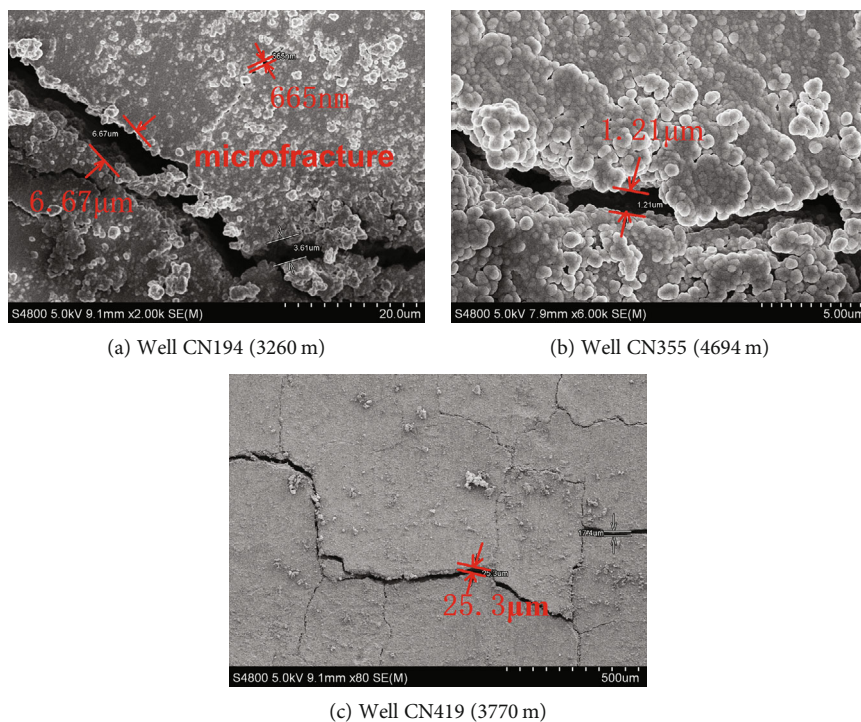


FIGURE 2: SEM images of rock samples of Wufeng Formation.

### 3. Results and Discussion

#### 3.1. Physicochemical Mechanism of Wellbore Instability in Longmaxi Formation and Wufeng Formation

##### 3.1.1. Fabric Analysis

(1) *Analysis of Mineral Composition.* Using the D/MAX-III A X-ray diffractometer, the relative contents of whole rock minerals and clay minerals in strata samples of the Longmaxi Formation and Wufeng Formation were determined. It can be seen from Table 2 that the rock samples of the Longmaxi

TABLE 4: Experimental data of hydration expansion.

Time (min)	Well no.							
	CN62	CN222	CN156	CN419	CN137	CN194	CN22	CN355
0	0	0	0	0	0	0	0	0
1	0.02	0.005	0	0.015	0	0.005	0.005	0.03
3	0.055	0.02	0.01	0.06	0.01	0.025	0.01	0.05
5	0.07	0.035	0.02	0.1	0.03	0.05	0.025	0.055
10	0.11	0.05	0.03	0.21	0.04	0.075	0.03	0.07
15	0.16	0.065	0.035	0.275	0.08	0.105	0.03	0.11
20	0.2	0.08	0.04	0.34	0.105	0.13	0.03	0.14
30	0.24	0.1	0.05	0.42	0.17	0.17	0.03	0.202
60	0.265	0.15	0.07	0.51	0.23	0.27	0.03	0.31
120	0.285	0.2	0.12	0.55	0.275	0.3	0.03	0.355
180	0.3	0.21	0.14	0.56	0.29	0.31	0.03	0.37
240	0.305	0.215	0.16	0.57	0.295	0.32	0.035	0.38
300	0.31	0.215	0.175	0.58	0.3	0.32	0.035	0.385
360	0.32	0.215	0.19	0.59	0.31	0.32	0.035	0.39
420	0.321	0.215	0.21	0.597	0.315	0.32	0.035	0.4
480	0.33	0.215	0.215	0.6	0.315	0.32	0.035	0.405
Core height (mm)	10.18	8.04	9.42	9.7	10.2	10	10.66	8.9
Swelling rate	3.24%	2.67%	2.28%	6.19%	3.09%	3.20%	0.33%	4.55%

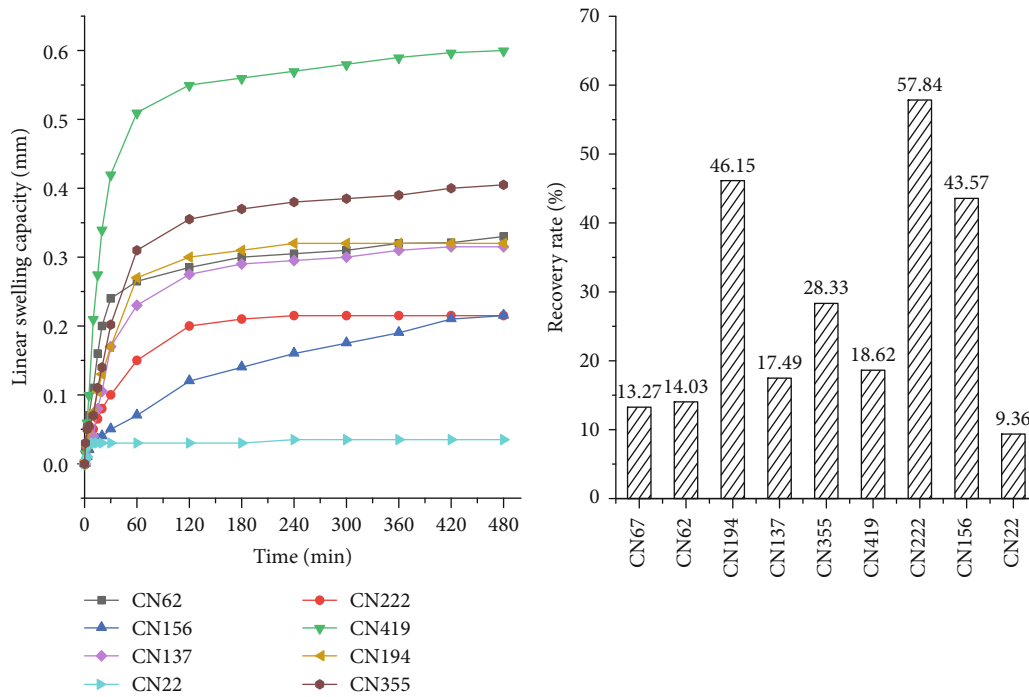


FIGURE 3: Test results of hydration swelling and dispersion properties of rock samples in Longmaxi Formation.

Formation are mainly quartz. The average content of quartz, calcite, barite, and clay minerals in the Longmaxi Formation is 32.46%, 19.85%, 13.54%, and 15.31%, respectively. The rock samples of the Wufeng Formation are mainly quartz, with quartz content of 33%, calcite content of 16.25%, barite content of 13.25%, and clay mineral content of 18%. It can be

seen from Table 3 that the clay minerals in the tested rock samples are mainly illite, but no kaolinite. The average content of illite, chlorite, and interlayer in the Longmaxi Formation is 57.46%, 21%, and 21.54%, respectively. The average content of illite, chlorite, and interlayer in the Wufeng Formation is 64%, 14.5%, and 21.5%, respectively.

TABLE 5: Experimental results of emulsifying agent optimization.

System	Condition	AV (mPa·s)	PV (mPa·s)	YP (Pa)	Gel10 <sup>''</sup> /Gel10 <sup>'</sup> (Pa/Pa)	FL <sub>API</sub> (mL)	Demulsification voltage (V)
Base slurry 1	Before aging	4.5	4	0.5	0.51/1.02	50.0	2047
	After aging	4	3	1	0.51/1.02	30.0	
EM-SL	Before aging	7	6	1	0	13.0	1101
	After aging	12	9	3	1.53/1.53	10.0	
EM-JH	Before aging	8	6	2	0	17.0	1012
	After aging	12	9	3	2.04/2.56	13.0	
EM-XG	Before aging	5.5	5	0.5	0	22.4	990
	After aging	12	9	3	1.53/1.53	18.0	

TABLE 6: Experimental results of filtrate reduces optimization.

System	Condition	AV (mPa·s)	PV (mPa·s)	YP (Pa)	Gel10 <sup>''</sup> /Gel10 <sup>'</sup> (Pa/Pa)	FL <sub>API</sub> (mL)
Base slurry 2	Before aging	7	6	1	0	13
	After aging	12	9	3	1.53/1.53	10
Lignite-SL	Before aging	10	9	1	1.02/1.53	8
	After aging	12.5	10	2.5	1.53/2.04	7.6
FR-BK	Before aging	12	11	1	1.02/2.04	2
	After aging	26.5	18	8.5	3.58/4.60	6.4
FR-JH	Before aging	10.5	9	1.5	1.02/1.53	9
	After aging	20.5	14	6.5	1.53/2.56	8

(2) *Characteristics of Microstructure.* The microstructure characteristics of strata samples of the Longmaxi Formation and Wufeng Formation were analysed by SEM. It can be seen from Figure 1 that the 3274 m sample of well CN194 has compact cementation, undeveloped intergranular pores, and dissolved pores. All samples of the Longmaxi Formation in well CN156 at 5100 m are fracture developed. Samples of the Wufeng Formation at 4694 m in well CN355 have developed fractures and pores. It can be seen from Figure 2 that fractures and dissolved pores and fractures are developed in the Wufeng Formation samples at 3260 m in well CN194. Samples of the Wufeng Formation at 4694 m in well CN355 have developed fractures and pores. The samples of the Wufeng Formation in well CN419 have compact cementation, undeveloped intergranular pores, and salt crystals in the cracks and crevices. The micropores of the Longmaxi Formation and Wufeng Formation are well developed, with a fracture width of 5~10  $\mu\text{m}$  and pore diameter of 400~900 nm. The apparent morphology of the shale is formed by discontinuous shale stacking and cementation, and the layered structure is obvious, which shows the characteristics of brittleness and low strength of shale.

### 3.1.2. Physical and Chemical Property Analysis

(1) *Hydration Properties.* In this experiment, rock samples from complex strata of each well are selected, shale dilatometer is used for the experiment, and water is used as the test

solution to test the hydration swelling properties of rock cores in complex sections of the Longmaxi Formation. The results are as follows.

Table 4 and Figure 3 show the analysis results of hydration properties of the Longmaxi Formation rock samples. It can be seen from Figure 3 that the swelling amount of the Longmaxi Formation rock samples is between 0.2 and 0.4 mm, most of which is above 0.3 mm, which has certain hydration swelling properties. It can be seen from the figure that the recovery rate of the Longmaxi Formation rock samples is between 9.36% and 57.84%, mostly below 30%, which has strong hydration and dispersion performance.

3.1.3. *Physicochemical Mechanism and Technical Countermeasures of Wellbore Instability.* Based on the analysis results of the fabric and the physical and chemical properties, the mechanism of wellbore instability of the Longmaxi Formation and Wufeng Formation in shale gas can be summarized as follows. On the one hand, clay content is high, mainly illite, no montmorillonite, and a small amount of illite/montmorillonite-mixed layer. Formation fractures and microfractures are developed, and formation hydration and dispersion are strong. On the other hand, the specific water affinity is large, and the drilling fluid filtrate intrudes into the deep part of the formation along the microfractures, causing hydration of shale. This leads to the weakening of

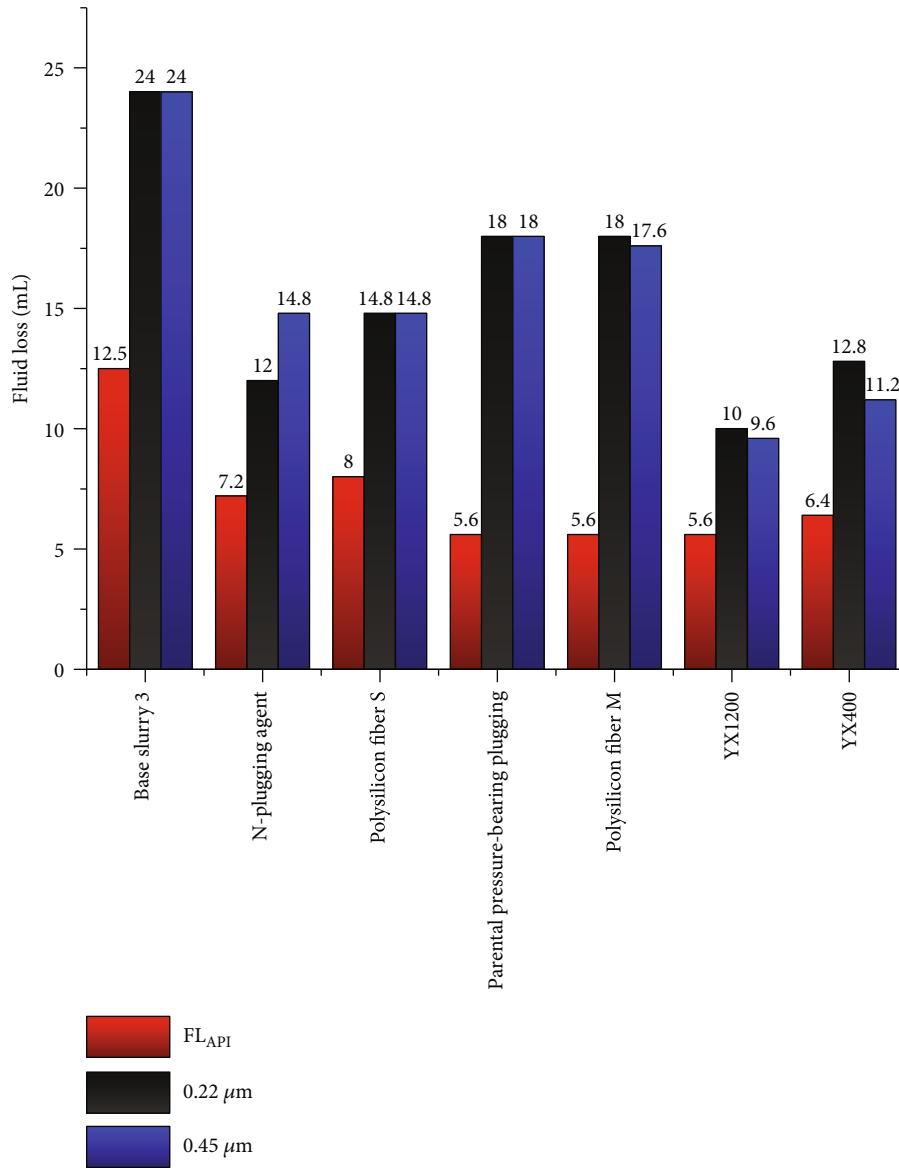


FIGURE 4: Experimental results of plugging agent optimization.

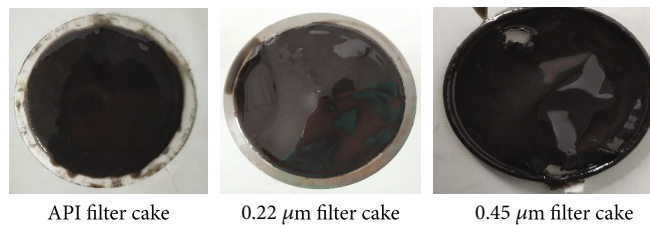


FIGURE 5: Picture of plugging agent YX1200 mud cake.

the cementation force between particles, and the expansion pressure produced by hydration makes the shaft lining lose balance, which leads to collapse and block falling.

According to the physicochemical mechanism and mechanical reasons of wellbore instability of the Longmaxi Formation and Wufeng Formation, the plugging technical

countermeasure of “strengthening plugging micropores, inhibiting filtrate invasion, and retarding pressure transmission” was put forward. In this technical countermeasure, the combination of physical and chemical plugging and effective stress-supporting shaft lining is emphasized, and the inhibition of surface hydration is strengthened. Strengthening the sealing

TABLE 7: Experimental results of lubricant optimization.

System	Condition	AV (mPa·s)	PV (mPa·s)	YP (Pa)	Gel10 <sup>''</sup> /Gel10 <sup>'</sup> (Pa/Pa)	FL <sub>API</sub> (mL)	Lubrication coefficient	Coefficient of viscosity
Base slurry 4	Before aging	12.5	11	1.5	1.02/1.53	5.5	0.0509	0.2493
	After aging	12	9	3	1.02/1.53	7.8		
Liquid rare earth	Before aging	12.5	9	3.5	1.02/1.53	5.6	0.0307	0.2309
	After aging	12	11	1	0.51/1.02	4.4		
Jiahua	Before aging	12	9	3	1.02/1.53	6	0.0305	0.2217
	After aging	13.5	11	2.5	1.53/1.53	6.4		
Graphite RT-1	Before aging	12.5	11	1.5	1.02/1.02	6	0.0205	0.1584
	After aging	12	9	3	1.02/1.53	7.6		

TABLE 8: Pollution resistance evaluation results of strong plugging drilling fluid.

System	Condition	AV (mPa·s)	PV (mPa·s)	YP (Pa)	Gel10 <sup>''</sup> /Gel10 <sup>'</sup> (Pa/Pa)	FL <sub>API</sub> (mL)	
Formula CN-5	NaCl resistance	Before aging	67.5	53	14.5	8.18/15.33	0.2
		125°C/16 h	77.5	59	18.5	3.58/25.55	0.2
	CaCl <sub>2</sub> resistance	Before aging	69	54	15	7.67/14.31	0.2
		125°C/16 h	80	65	15	3.58/22.98	0
	Poor clay resistance	Before aging	67.5	52	15.5	8.18/15.33	0
		125°C/16 h	73	58	15	7.15/18.40	0

TABLE 9: Temperature resistance evaluation results of strong plugging drilling fluid.

System	Condition	AV (mPa·s)	PV (mPa·s)	YP (Pa)	Gel10 <sup>''</sup> /Gel10 <sup>'</sup> (Pa/Pa)	FL <sub>API</sub> (mL)	
Formula CN-5	Temperature resistance	Before aging	67.5	52	15.5	8.18/15.33	0.2
		135°C/16 h	75	60	15	3.58/23.51	0
	Temperature endurance	Before aging	67.5	52	15.5	8.18/15.33	0.2
		125°C/32 h	78	64	14	10.22/15.33	0

TABLE 10: Stability evaluation results of strong plugging drilling fluid.

System	Improved VST settlement test method				Settlement stability	Electrical stability	
Formula	Volume (mL)	Mass (g)		Density difference (g/mL)	Density difference between upper and lower layers (g/mL)	Demulsification voltage (V)	
CN-5		600r	100r	The difference			
	10	19.42	20.06	0.64	0.064	0.019	1322

to prevent and slow down pore pressure transmission is the premise of improving the effective mechanical support of the downhole liquid column pressure to the wellbore, further establishing effective stress support for shaft lining to balance the collapse pressure of the shaft lining.

### 3.2. Enhanced Plugging Drilling Fluid and Its Performance

#### 3.2.1. Evaluation and Optimization of Key Additives for Oil-Based Drilling Fluid

(1) *Optimization of Emulsifier.* Taking “360 mL white oil + 3% organic bentonite + 40 mL CaCl<sub>2</sub> brine (25%)” as the

base slurry 1, the rheological properties (including shear force), filtration, and demulsification voltage of each experimental slurry (base slurry 1 + main emulsifier 4% + auxiliary emulsifier 2%) before and after hot rolling at 125°C for 16 hours were tested. It can be seen from Table 5 that the demulsification voltage of each experimental pulp after hot rolling at 125°C/16 h is greater than 400 V, and the system is stable. Emulsifier is not added in the base slurry, and no emulsion is formed, so the demulsification voltage of the base slurry is 2047 V. The better the emulsification effect, the more uniform the dispersion of water-in-oil emulsion, the higher the apparent viscosity of drilling fluid, and the higher the apparent viscosity of emulsifier EM-SL experimental slurry, with



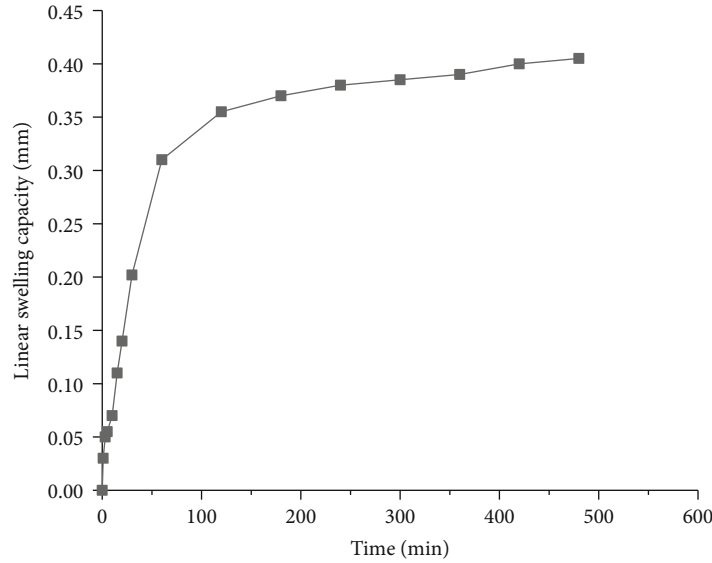


FIGURE 6: Experimental results linear swelling experiment.

TABLE 11: Hot-rolling dispersion experiment.

System	Before dispersion (g)	After dispersion (g)	Rete of recovery (%)
Formula CN-5	30	29.81	99.37

the lowest filtration loss, so the emulsifier constructed by the formula is preferred.

(2) *Optimization of Fluid Loss Reducer.* With “360 mL white oil + 3% organic bentonite + 4% main emulsifier + 2% auxiliary emulsifier + 40 mL CaCl<sub>2</sub> brine (25%)” as base slurry 2, the rheological properties of each experimental slurry (base slurry 2 + 2% fluid loss additive) before and after hot rolling at 125°C for 16 hours were tested. The experimental results in Table 6 show that the apparent viscosity after aging is improved in different degrees than before, and the fluid loss after adding the fluid loss reducer FR-BK is 6.4 mL, and the fluid loss is the lowest among the preferred treatment agents. Moreover, it has a certain viscosity and shear force, which is helpful to the suspension of cuttings and has excellent rheological properties, so the fluid loss reducer constructed by the formula is preferred.

(3) *Optimization of Plugging Agent.* According to the characteristics of microcracks and micropores in the Longmaxi Formation rock samples, N-plugging agents, YX1200 and YX400, and other micro-nanoplugging agents were researched and selected, and 0.22 μm and 0.45 μm microfiltration membranes were introduced to evaluate the pressure-bearing plugging ability of the plugging agents. With “360 mL white oil + 3% organic bentonite + 4% main emulsifier + 2% auxiliary emulsifier + 40 mL CaCl<sub>2</sub> brine + 2% oil-based lignite-SL” as base slurry 3, the experimental slurry (base slurry 3 + 5% plugging agent) was tested before and after hot rolling at 125°C for 16 hours. It can be seen

from Figures 4 and 5 that the API filtration loss of experimental slurry with the YX1200 plugging agent is 5.6 mL, and the filtration loss through microporous membranes with pore diameters of 0.22 μm and 0.45 μm is 10 mL and 9.6 mL, respectively. Compared with other plugging agents, the YX1200 plugging agent has the lowest filtration loss and better plugging effect, so it is selected as the plugging agent for the oil-based drilling fluid.

(4) *Optimization of Lubricant.* With “360 mL white oil + 3% organic bentonite + 4% main emulsifier + 2% auxiliary emulsifier + 40 mL CaCl<sub>2</sub> brine + 2% oil-based lignite-SL + 5% plugging agent YX1200” as base slurry 4, each experimental slurry (base slurry + 1.5% lubricant) was tested. The experimental results in Table 7 show that the lubricating coefficient and viscosity coefficient of the experimental slurry added with solid lubricant-BK are 0.0102 and 0.1495, respectively, which are lower than those of other lubricants. The graphite RT-1 was selected as the lubricant for the next experiment.

3.2.2. *Performance Evaluation of Enhanced Plugging Drilling Fluid.* By further optimizing the organic bentonite, plugging agent, and viscosity reducer and optimizing the compatibility of the system, an enhanced plugging drilling fluid system was constructed. It consists of 360 mL white oil + 4% organic bentonite (BK) + 4% main emulsifier (EM-SL) + 2% auxiliary emulsifier (EM-SL) + 4% wetting agent + 2% quicklime + 40 mL CaCl<sub>2</sub> brine + 4% oil-based fluid loss reducer (BK) + 4% plugging agent (YX1200) + 1.0% solid lubricant RT-1 + 1.5% flow pattern regulator + barite (the density is adjusted to 1.5 g/cm<sup>3</sup>), which is designated as Formula CN-5.

(1) *Contamination Resistibility.* By adding 10% NaCl, 1.0% CaCl<sub>2</sub>, and 8% poor clay (passing through 100-mesh sieve) into the Formula CN-5 drilling fluid system, the antipollution ability of each system is evaluated by observing the

TABLE 12: Fracture sealing evaluation results of strong plugging drilling fluid.

System	Leaking bed	Pressure bearing time (min)	Leakage stoppage		Description of plugging of leakage bed
			Pressure (MPa)	Accumulated leakage (mL)	
Formula CN-5	400 $\mu\text{m}$ crack block	3	0	0	There was no drilling fluid leakage during the experiment
		3	0.5	0	
		3	1.0	0	
		3	2.0	0	
		3	3.0	0	
		3	4.0	0	
		3	5.0	0	

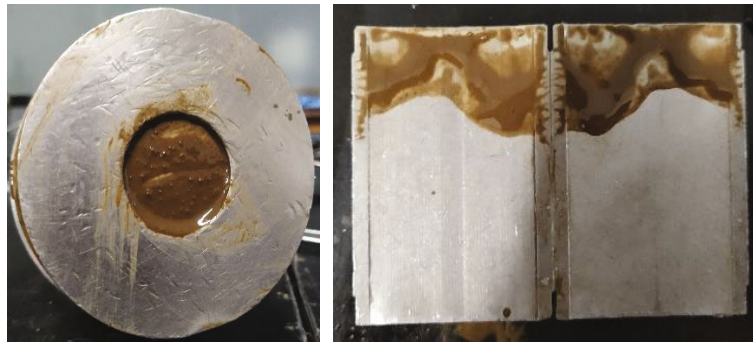


FIGURE 7: Fracture sealing evaluation results of strong plugging drilling fluid. Evaluation of leakage and plugging performance of 400  $\mu\text{m}$  microfractures with Formula CN-5 drilling fluid.

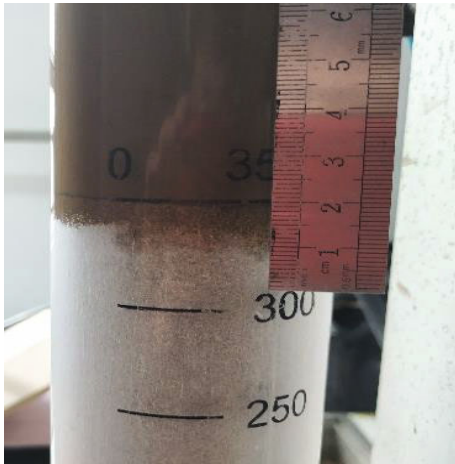


FIGURE 8: Sealing sand bed test results of strong plugging drilling fluid.

performance changes before and after hot rolling at 125°C for 16 hours. The evaluation results are shown in Table 8.

The experimental data in Table 8 show that after adding 10% NaCl into the Formula CN-5 drilling fluid system, the apparent viscosity of the system has little change, and its salt resistance is better. After adding 8% poor clay and 1.0% calcium chloride, the viscosity increased slightly, and it had certain poor clay resistibility and calcium resistibility.

(2) *Performance of Temperature Resistance.* The rheological properties and fluid loss of Formula CN-5 before and after hot rolling at 135°C for 16 hours and 125°C for 32 hours were tested.

It can be seen from Table 9 that the rheological fluid loss of the Formula CN-5 drilling fluid system has little change after hot rolling, which indicates that they have excellent temperature resistance.

(3) *Stability.* The settlement stability, electrical stability, and improved VST settlement of Formula CN-5 were tested. The experimental results are shown in Table 10.

The experimental results show that the Formula CN-5 drilling fluid has good dynamic settlement stability, with a density difference of 0.064 g/mL, density difference between upper and lower layers of 0.019 g/mL, and demulsification voltage of 1322 V, which is more than 400 V, which indicates that the system is stable.

(4) *Inhibition.*

(a) *Linear swelling experiment:* rock cuttings passing through 100 meshes in the Longmaxi Formation of CN22 well are selected, and the hydration and expansion properties of the core in the complex section of the Longmaxi Formation are tested by linear swelling experiment and Formula CN-5 drilling fluid as the test solution. The results are shown in Figure 6.

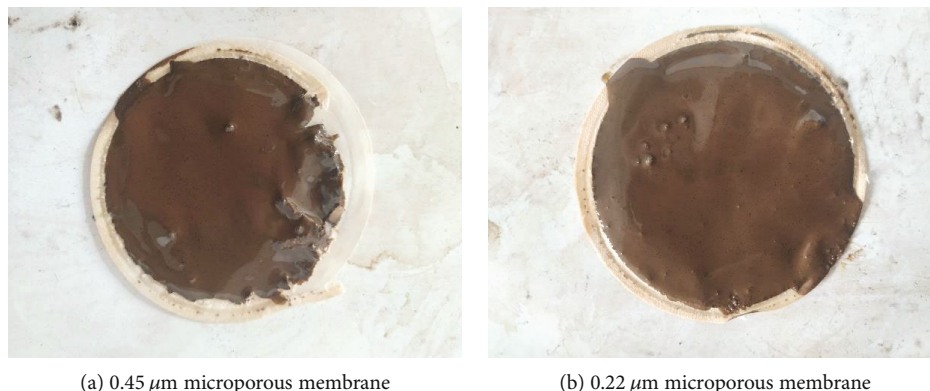


FIGURE 9: Experimental results of microporous filter test.

(b) *Hot-rolling dispersion experiment*: rock cuttings passing 2-5 mm mesh in the CN22 well of the Longmaxi Formation were selected, and the hydration and dispersion inhibition performance of the Formula CN-5 drilling fluid was evaluated by the hot-rolling dispersion experiment. The results are shown in Table 11.

It can be seen from Figure 6 and Table 10 that the Formula CN-5 drilling fluid system has a small hydration expansion amount, and the rolling recovery rate of cuttings is greater than 95%, indicating that the drilling fluid system still has a strong ability to inhibit hydration expansion and hydration dispersion.

#### (5) Performance of Leakage Prevention and Plugging.

(a) *Evaluation of plugging performance of fractured leakage*: using a high-temperature and high-pressure (HTHP) plugging simulation experimental device, the plugging and bearing capacity of Formula CN-5 drilling fluid to 400  $\mu\text{m}$  microcracks is evaluated. The experimental results are shown in Table 12 and Figure 7.

The Formula CN-5 drilling fluid system has a certain plugging ability for 400  $\mu\text{m}$  fractures, and there is no leakage during the experiment, and the average invasion depth is shallow.

(b) *Evaluation of permeability leakage plugging performance*: through sealing of the sand bed instrument, 40-60-mesh sieve fine sand is selected to evaluate the leakage prevention performance of optimized drilling fluid permeability leakage. The experimental results are shown in Figure 8. According to the analysis of sand bed plugging experiment results, the average invasion depth of the Formula CN-5 drilling fluid system is 7 mm, and the invasion is shallow, which has strong permeability plugging performance.

(c) *Experimental method for plugging evaluation of micro-nanopores and fractures*: according to the characteristics of micro-nanopores and fractures in shale formation, the plugging ability of the Formula CN-5 oil-based drilling fluid was tested by using a microporous filter membrane instead of API filter paper to simulate the fracture and micropore, and the lost volume and bearing capacity were taken as evaluation indexes. The experimental results show that the instantaneous filtration loss of the Formula CN-5 drilling fluid is 0 mL after 0.45  $\mu\text{m}$  and 0.22  $\mu\text{m}$  microporous membrane evaluation systems, and the filtration loss is still 0 mL after 30 min. The mud cake produced by the microporous membrane is shown in Figure 9. Experiments show that the Formula CN-5 drilling fluid system has certain ability of plugging microcracks and micropores.

As discussed before, mineral composition analysis shows that the rock samples of the Longmaxi Formation are mainly quartz, with an average content of 32.46%, calcite 19.85%, and clay mineral 15.31%. The rock samples of the Wufeng Formation are mainly quartz, with an average content of 33%, calcite content of 16.25%, and clay mineral content of 18%. The microstructure analysis shows that the rock samples of the Longmaxi Formation have compact cementation, and the intergranular pores do not develop, but there are cracks and dissolution pores and fractures, and occasionally, there are salt crystals in the pores. Hydration swelling and dispersion tests show that the hydration swelling rate of Longmaxi Formation rock samples in 8 wells in the field is 3.3% on average, with weak swelling, and the dispersion recovery rate of Longmaxi Formation rock samples is 27.63% on average, with strong dispersion.

Based on the analysis of well conditions and drilling fluid performance of each well, in order to reduce downhole sticking and drilling leakage, the functional indexes of oil-based drilling fluid in the Changning block are preliminarily recommended as follows: shale expansion rate is controlled below 0.25%, lubrication coefficient is controlled below 0.040, shale recovery rate is controlled above 99% (different

rock samples will vary), sand bed invasion depth is controlled below 12 mm, and bearing capacity for 200  $\mu\text{m}$  and 400  $\mu\text{m}$  fractures is greater than 5 MPa.

The constructed oil-based drilling fluid system “360 mL white oil + 4% organic bentonite (BK) + 4% main emulsifier (EM-SL) + 2% auxiliary emulsifier (EM-SL) + 4% wetting agent + 2% quicklime + 40 mL  $\text{CaCl}_2$  brine + 4% oil-based fluid loss reducer (BK) + 4% plugging agent (YX1200) + 1.0% solid lubricant RT-1 + 1.5% flow pattern regulator + barite (the density is adjusted to 1.5  $\text{g}/\text{cm}^3$ )” in the Changning block is stable and easy to maintain and control.

Due to the addition of micron-sized plugging materials, it has certain plugging ability for microcracks and micropores. If you want the oil-based drilling fluid system to have better plugging and anticollapse performance, the plugging agent of the oil-based drilling fluid should be selected from lipophilic micro-nanomaterials, and the experimental methods and means for evaluating micro-nanomaterials should be further developed.

#### 4. Conclusion

In this paper, the causes of wellbore instability of shale gas horizontal section in the Changning block are analysed, and the corresponding solutions are put forward. A set of experimental methods for evaluating oil-based drilling fluid system is summarized, and a set of an oil-based drilling fluid system suitable for shale formation with microfracture development is constructed. The Longmaxi Formation and Wufeng Formation are hard and brittle shales mainly composed of illite, with developed microfractures and strong hydration of some formations. When the drilling fluid filtrate deeply intrudes into the formation along the microfractures, it will cause hydration of shale, which weakens the cementation force between particles, while hydration stress caused by hydration makes the wellbore lose balance, resulting in complex situations such as wellbore dropping and collapse. Besides, this paper puts forward the plugging theory of “strengthening plugging micropores, inhibiting filtrate invasion, and retarding pressure transmission.” It emphasizes the combination of physical and chemical plugging and effective stress supporting of the wellbore and enhanced inhibition of surface hydration. Strengthening the sealing to prevent and slow down of pore pressure transmission is the premise of improving the effective mechanical support of downhole liquid column pressure to the wellbore. Effective stress needs to be further established to support the shaft lining to balance the collapse pressure of the shaft lining. Finally, the shale gas oil-based drilling fluid system constructed in this paper has strong plugging ability, excellent inhibition and temperature resistance, preferable contamination resistibility, and good rheological property and filtration wall-building property and is easy to control.

#### Nomenclature

AV: Apparent viscosity (mPa·s)  
 PV: Plastic viscosity (mPa·s)

YP: Yield point (Pa)  
 $\text{FL}_{\text{API}}$ : API filtration (mL).

#### Data Availability

The experimental data used in this paper are true and effective, and all come from experimental research.

#### Conflicts of Interest

The authors declare that they have no conflicts of interest.

#### Acknowledgments

This work was financially supported by the National Natural Science Foundation of China (No. 51974351; No. 51704322; Major Program, No. 51991361), the National Science and Technology Major Project of China (No. 2016ZX05040-005), and PCSIRT (IRT\_14R58).

#### References

- [1] X. Ma and J. Xie, “Shale gas exploration and development progress and development prospect in southern Sichuan,” *Petroleum Exploration and Development*, vol. 45, no. 1, pp. 161–169, 2018.
- [2] F. Pengfei, *Study on the collapse and instability mechanism of shale horizontal wells in WY-CN Longmaxi formation*, Southwest Petroleum University, 2016.
- [3] L. Jingping and S. Jinsheng, “Hydration instability mechanism and inhibition method of shale gas reservoir formation,” *Drilling Fluid and Completion Fluid*, vol. 33, no. 3, pp. 25–29, 2016.
- [4] C. Cao, M. Zhang, L. Li et al., “Tracing the sources and evolution processes of shale gas by coupling stable (c,H) and noble gas isotopic compositions: cases from Weiyuan and changing in Sichuan basin, China,” *Journal of Natural Gas Science and Engineering*, vol. 78, no. 5, pp. 23–26, 2020.
- [5] X. Wang, B. Dongqing, S. Yunchao et al., “All-oil-based drilling fluid system for enhanced plugging of shale gas wells — taking Weiyuan block in Changning-Weiyuan National Shale Gas Demonstration Zone as an example,” *Natural Gas Industry*, vol. 40, no. 6, pp. 107–114, 2020.
- [6] L. Liang, Z. Dalin, L. Xiangjun et al., “Study on mechanical properties and failure modes of Longmaxi formation shale,” *Chinese Journal of Underground Space and Engineering*, vol. 13, no. 1, pp. 108–116, 2017.
- [7] S. Jinsheng, L. Jingping, Y. Lili et al., “Present situation of shale gas well water-based drilling fluid technology at home and abroad and development direction in China,” *Drilling Fluid and Completion Fluid*, vol. 33, no. 5, pp. 1–8, 2016.
- [8] H. C. H. Dreley, “A laboratory investigation of borehole stability,” *Journal of Technology*, vol. 21, no. 7, pp. 883–892, 1969.
- [9] X. Chen, C. P. Tan, and C. Detournay, “A study on wellbore stability in fractured rock masses with impact of mud infiltration,” *Journal of Petroleum Science and Engineering*, vol. 38, no. 3–4, pp. 145–154, 2003.
- [10] X. Chen, Q. Yang, K. B. Qiu, and J. L. Feng, “An anisotropic strength criterion for jointed rock masses and its application in wellbore stability analyses,” *International Journal for Numerical and Analytical Methods in Geomechanics*, vol. 32, no. 6, pp. 607–631, 2008.

- [11] J. Zhang, "Borehole stability analysis accounting for anisotropic in drilling to weak bedding planes," *International Journal of Rock Mechanics and Mining Sciences*, vol. 22, no. 3, pp. 160–170, 2013.
- [12] O. Gaede, F. Karpfinger, J. Jocker, and R. Prioul, "Comparison between analytical and 3D finite element solutions for borehole stresses in anisotropic elastic rock," *International Journal of Rock Mechanics and Mining Sciences*, vol. 51, pp. 53–63, 2012.
- [13] Z. Haifeng, Y. Wang, and F. Fan, "Oil-based drilling fluid technology for strong plugging of shale gas horizontal wells," *Natural Gas Technology and Economics*, vol. 12, no. 5, pp. 33–36, 2018.
- [14] Z. Feng, Z. Yang, and S. Luo, "Drilling difficulties and countermeasures in Changning shale gas horizontal section," *Drilling and Production Technology*, vol. 43, Supplement 1, pp. 4–7, 2020.
- [15] T. Guowang, G. Weichao, and P. Yu, "Research and application of strong plugging oil-based drilling fluid system," *Prospecting Engineering (Geotechnical Drilling and Excavation Engineering)*, vol. 44, no. 11, pp. 21–25, 2017.
- [16] W. Yinwu and Z. Xue, "Application of oil-based drilling fluid technology in shale gas wells in western Sichuan," *Liaoning Chemical Industry*, vol. 45, no. 6, pp. 773–776, 2016.
- [17] Z. Gaobo, Q. Gao, and Q. Ma, "Measures to improve the anti-collapse performance of oil-based drilling fluid in shale gas formation," *Drilling Fluid and Completion Fluid*, vol. 36, no. 2, pp. 141–147, 2019.
- [18] M. Meng, Z. Zamanipour, S. Miska, M. Yu, and E. M. Ozbayoglu, "Dynamic stress distribution around the wellbore influenced by surge/swab pressure," *Journal of Petroleum Science and Engineering*, vol. 172, pp. 1077–1091, 2019.
- [19] Z. Hanyi, Q. Zhengsong, H. Wei'an et al., "Development and features of amine shale inhibitors," *Petroleum Drilling Techniques*, vol. 38, no. 1, pp. 104–108, 2010.
- [20] Z. Hanyi, Q. Zhengsong, H. Wei'an, F. W. Wang, and X. B. Zhang, "Experimental evaluation on polyamine water-based drilling fluid," *Oilfield Chemistry*, vol. 27, no. 2, pp. 119–123, 2010.
- [21] J.-g. Xu, Z. Qiu, X. Zhao, H. Zhong, and W. Huang, "Study of 1-octyl-3-methylimidazolium bromide for inhibiting shale hydration and dispersion," *Journal of Petroleum Science and Engineering*, vol. 177, no. 2, pp. 208–214, 2019.